

# Enhancement inhibition efficiency of PBTCA depending on the inclusion complex with hydroxypropyl- $\beta$ -cyclodextrin

Chang Jun Zou · Quan Wu Tang · Gui Hong Lan ·  
Qiang Tian · Tai Yu Wang

Received: 12 July 2011 / Accepted: 3 May 2012 / Published online: 9 June 2012  
© Springer Science+Business Media B.V. 2012

**Abstract** For the first time, hydroxypropyl- $\beta$ -cyclodextrin (HP- $\beta$ -CD) has been brought in to include 2-phosphonobutane-1,2,4-tricarboxylic acid (PBTCA) in order to enhance inhibition efficiency of PBTCA, which leads a new approach to study oil–gas field corrosion inhibition in the process of acid treatment. Based on the host–guest inclusion reaction, the inclusion complex of PBTCA with HP- $\beta$ -CD has been prepared in the laboratory. UV–Vis absorption spectrum was applied to study the inclusion behavior of PBTCA with HP- $\beta$ -CD. The results revealed that PBTCA with HP- $\beta$ -CD can form a 1:1 stoichiometry inclusion complex. The 1:1 inclusion complex synthesized by using lyophilization was further characterized by Fourier transform infrared spectroscopy. Besides, inhibition effect of the inclusion complex on the corrosion inhibition of Q235 carbon steel has been investigated in 0.1 M sulfuric acid ( $\text{H}_2\text{SO}_4$ ) solution using potentiodynamic polarization, electrochemical impedance spectroscopy techniques and scanning electron microscopy (SEM). It was found that the presence of the inclusion complex better achieved the anti-corrosion property in aggressive medium than was the case with alone PBTCA and the highest inhibition efficiency of the inclusion complex over 90 % was obtained, which are suggestive of the active effect of the inclusion complex for improving inhibition efficiency of

PBTCA. Meanwhile, the results obtained from SEM further showed that the inclusion complex acts as a more efficient corrosion inhibitor for Q235 carbon steel in  $\text{H}_2\text{SO}_4$  medium.

**Keywords** Corrosion · Corrosion inhibitor · Hydroxypropyl- $\beta$ -cyclodextrin · Inclusion complex · PBTCA

## Introduction

2-Phosphonobutane-1,2,4-tricarboxylic acid (PBTCA, Fig. 1), an important member of organic phosphonic acids family, is an environment-friendly agent which has a wide range of applications such as scale inhibition of calcium carbonate, chemical mechanical polishing of copper and corrosion inhibition of carbon steel, etc. [1–3]. In this paper, with the purpose of reducing corrosive rate of steel, PBTCA injected into the corrosive medium as a corrosion inhibitor has been employed in the application of corrosion inhibition. Actually, corrosion inhibitor technology is an effective and economic way for protecting metal from corrosion [4–10], which has been widely used in many industries, especially in the oil–gas field development. More particularly, as is well known, the use of alone PBTCA could hardly get the desired anti-corrosion performance, which has restricted its further application. Generally, however, some important ways which could effectively improve inhibition efficiency of organic phosphonic acid as corrosion inhibitor have been reported. For instance, organic phosphonic acid in association with different metal ions like  $\text{Ca}^{2+}$ ,  $\text{Zn}^{2+}$ , etc., has been applied in the cooling water systems [11–15]. Moreover, it has been proposed that organic phosphonic acid combined with a bivalent metal cation such as  $\text{Zn}^{2+}$  and polyoxyethylene

C. J. Zou (✉) · Q. W. Tang · G. H. Lan  
Department of Chemistry and Chemical Engineering, Southwest  
Petroleum University, Chengdu, China  
e-mail: changjunzou@126.com

Q. Tian  
Yunnan Chemical Research Institute, Yunnan, China

T. Y. Wang  
Liaohe Oilfield Co, PetroChina, Panjin, China

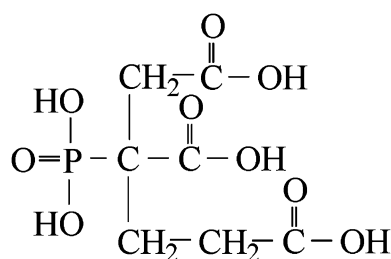


**Fig. 1** The chemical structure of PBTCA

sorbitan monooleate [16], some co-inhibitors like *N*-cetyl *N,N,N*-trimethyl ammonium bromide or *N*-cetyl pyridinium chloride [17]. Nevertheless, a new high performance and environment-friendly approach to improve inhibition efficiency of PBTCA, based on host–guest inclusion interaction, will be presented in this paper.

Cyclodextrins (CDs) as one of the most prominent host molecules [18–23], have been extensively investigated. Many of inorganic or organic guest molecules can be fully or partly incorporated into the cavities of CDs to form inclusion complexes because of their unique cavity of hydrophobic interior and polar or hydrophilic exterior. The formation of inclusion complex can modify the physical and chemical properties of guest molecules. The host–guest inclusion complex can sustain the release rate of drugs [24], enhance the peak concentration of drugs in blood [25], and improve bioavailability [26], etc., which have been widely reported.

It was presented, in our previous work [27] that the inclusion complex of PBTCA with  $\beta$ -CD has its potential application to enhance oil production in reservoirs. Whereas, natural  $\beta$ -CDs have limited water solubility. In contrast, some chemically derivatives of CDs obtain a significant increase in water solubility, which have been synthesized by derivatization of the free hydroxyl groups of the CDs with alkyl and sulfobutyl groups resulting in hydroxyalkyl, methyl, and sulfobutyl derivatives with higher water solubility [28]. The present study will further extend the use of hydroxypropyl- $\beta$ -cyclodextrins (HP- $\beta$ -CDs) to the application of oil–gas field.

The current work aims to study the inclusion behavior and anti-corrosion performance of PBTCA in HP- $\beta$ -CD complexes, under the condition of laboratory. UV–Vis absorption spectrum was applied to study an inclusion complex formation in solution. For this purpose corrosion inhibitor: the inclusion complexes were synthesized by lyophilization and characterized by Fourier transform infrared spectroscopy (FTIR). Furthermore, the corrosion behavior of Q235 carbon steel samples in 0.1 M  $H_2SO_4$  solution without and with the inclusion complex was investigated by the potentiodynamic polarization, electrochemical impedance spectroscopy (EIS) techniques and scanning electron microscopy (SEM).

## Experimental

### Materials

HP- $\beta$ -CD (DS: 6.0) was purchased from Tianjin Chemical Factory (Tianjin, China). PBTCA, concentrated sulfuric acid ( $H_2SO_4$ ), sodium hydroxide, anhydrous ethanol and potassium chloride (KCl) were obtained from Chengdu Zhangzheng Huabo Chemical Reagent Co. Ltd (Chengdu, China). All reagents were of analytical reagent grade or much better. Doubly distilled water was used throughout. Electrochemical tests were performed on a Q235 carbon steel of the following chemical composition (wt%): C (0.14–0.22), Mn (0.30–0.65), Si ( $\leq 0.30$ ), S ( $\leq 0.05$ ), P ( $\leq 0.045$ ), and the remainder iron.

### Preparation of the inclusion complex of PBTCA with HP- $\beta$ -CD

Preparation of the inclusion complex of PBTCA with HP- $\beta$ -CD was performed according to the method described previously [27]. Aqueous solution containing PBTCA and HP- $\beta$ -CD, in a different molar ratio was obtained by dissolving HP- $\beta$ -CDs in distilled water. All experiments were carried out under the atmospheric ambient, the reacting temperature at  $40 \pm 1$  °C was controlled by electro-thermostatic water bath (Nanjing Instrumentation Manufacture Co., Ltd, China), the stir speed was restricted at 150 r/min and the reaction time continued for 12 h. UV–Vis absorption spectrum (Shanghai Spectrotech Instruments Co., Ltd, China) was applied to study the inclusion behavior at room temperature (25 °C). The solid inclusion complexes were prepared by freeze drying method.

### FTIR

PBTCA, HP- $\beta$ -CD, and the inclusion complex of PBTCA with HP- $\beta$ -CD spectra were recorded by using a Nicolet 170SX spectrometer (Nicolet, USA). Spectra acquisitions were performed directly in powder samples with the application of 16 scans at a resolution of  $4\text{ cm}^{-1}$  over the range  $4,000\text{--}400\text{ cm}^{-1}$ .

### Electrochemical experiments

Prior to all experimental measurements, the Q235 carbon steel specimens were ground with different emery papers (grade 400, 600, 800, 1,000, and 1,200), rinsed with double distilled water, degreased in absolute ethanol, and dried by compressed air at room temperature (25 °C). Appropriate concentrations of acid and corrosion inhibitor were prepared using double distilled water. The corrosive solutions were made of AR grade 95 %  $H_2SO_4$  and the concentration was 0.1 M. The concentration range of the inclusion

complex employed was 80–100 mg/L in the acid solution. Required the concentration of PBTCa was identical with the inclusion complex.

Electrochemical experiments were performed using a computer-controlled system CHI 604D (Shanghai chenhua Instrument Co. Ltd, China). Carrying out the whole process of these, a three-electrode arrangement was used for electrochemical studies. The homemade working electrode was prepared from a Q235 carbon steel sheet, mounted in polyester so that the area exposed to the aggressive solution was 1 cm<sup>2</sup>. The reference electrode was a saturated calomel electrode, which was separated from the solution by a bridge compartment filled with the saturated solution of potassium chloride (KCl). A platinum disc electrode was used as a counter electrode. For potentiodynamic polarization measurements, the polarization curve was performed at a scan rate of 0.3 mV·s<sup>-1</sup>. The impedance measurements were carried out in the frequency range of 100 kHz to 0.05 Hz at the open circuit potential, by applying an amplitude vibration of 5 mV sine wave ac voltage. The immersion time before each test was 60 min to access an equilibrium potential.

All experiments were performed under the atmospheric ambient, the temperature at 25 ± 1 °C was controlled by electro-thermostatic water bath. The polarization curve and the EIS were both calculated by ZView software.

#### Corrosion attack morphology studies

In order to investigate the inhibition effect of the corrosion inhibitor on corrosion morphology, SEM has been employed in this study. The surface morphology of the corrosion products formed on the surface of the Q235 carbon steel samples in 0.1 M H<sub>2</sub>SO<sub>4</sub> solutions without and with the corrosion inhibitor were recorded at 24 h immersion time by SEM examinations using a Philips XL30-EDAX electron microscope (Philips, Holland).

## Results and discussion

### UV–Vis spectroscopy

UV–Vis absorption spectra for the pure PBTCa and the inclusion complex with different molar ratios (Fig. 2) have been studied in distilled water. The results of UV–Vis spectra show the absorption spectrum of inclusion complexes aqueous solution coincides with the pure PBTCa at 215–240 nm, the maximum peaks appears at 221.5 nm, and the absorbance of the PBTCa solution increases with the addition of HP-β-CD. The similarity of the changes indicates that the inclusion complexes have formed between HP-β-CD and PBTCa and also suggests the

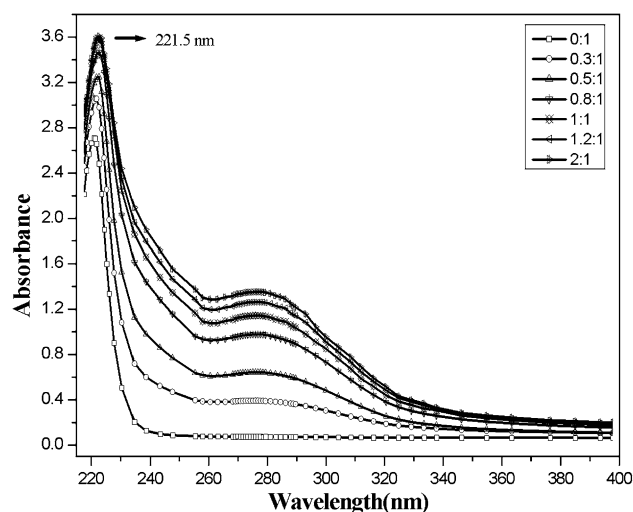


**Fig. 2** UV–Vis spectra of PBTCa in HP-β-CD aqueous solution with different mole ratio ([HP-β-CD]/[PBTCa])

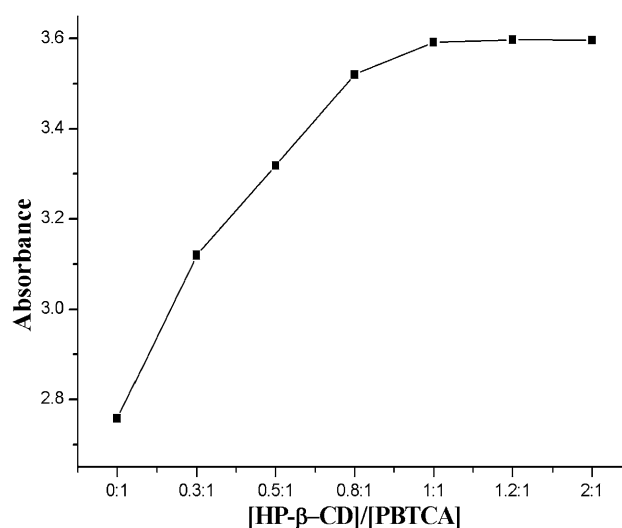


**Fig. 3** Absorbance of [HP-β-CD]/[PBTCa] solution at different mol ratio at 221.5 nm

inclusion mechanism of HP-β-CD with PBTCa is similar for the previous analyzed of β-CD [27].

The inclusion ratio has been confirmed by using the changes of the absorbance value of the solution. With the concentration of inclusion complex increasing, the absorbance value of the solution at a wavelength of 221.5 nm (Fig. 3) rises more and more slowly. When the molar ratio proportion of HP-β-CD to PBTCa reaches 1:1, the absorbance value yields to stationary. Therefore, the applicable inclusion ratio of inclusion complexes is 1:1.

The host–guest inclusion reaction of CD in aqueous solution characterized a dynamic and equilibrium process conforms to mass action law. The apparent inclusion constant ( $K$ ) could be calculated as Eq. 1, according to the Hildebrand–Benesi formula of the type of 1:1 [29].

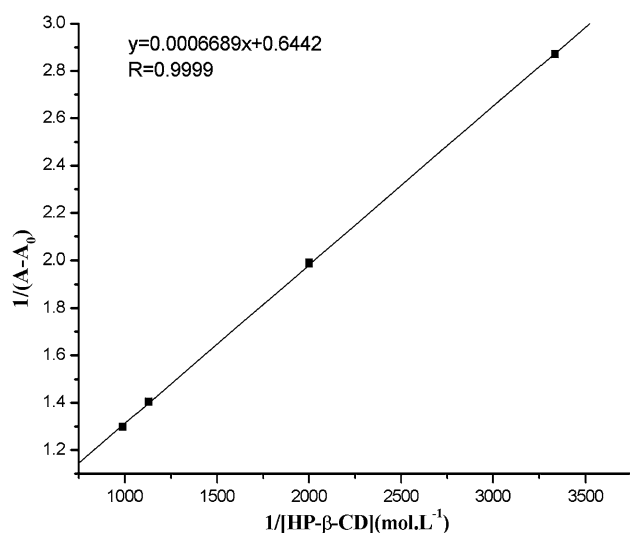


**Fig. 4** Double reciprocal plot for the inclusion complex of PBTCa with HP-β-CD at 25 °C

$$\frac{1}{A - A_0} = \frac{I}{K[CD]_0} + I \quad (1)$$

Where  $K$  is the apparent inclusion constant;  $[CD]_0$  is the initial concentration of HP-β-CD in the solution;  $A_0$  and  $A$  is the absorbance value of the free guest and the guest with host HP-β-CD, respectively; and  $I$  is the intercept.

A double reciprocal plot for the inclusion complex of PBTCa with HP-β-CD (Fig. 4) is obtained by plotting the value of  $1/(A - A_0)$  versus  $1/[CD]_0$ . The apparent inclusion constant ( $K$ ) is the value of ratio of the intercept and slope of the straight line and the calculated  $K$  value was 963.1 at 25 °C.

## FTIR

FTIR was used to characterize the structures of the free guest PBTCa, hosts HP-β-CD and the inclusion complex. FTIR spectrum of inclusion complex (Fig. 5) shows changes from parent spectra (i.e., pure PBTCa and HP-β-CDs). The obtained FTIR data supports the formation the inclusion complex.

The PBTCa FTIR spectrum shows the presence of the characteristic peaks: 3,450  $\text{cm}^{-1}$  (–OH); 1,720  $\text{cm}^{-1}$  (–C=O); 1,411  $\text{cm}^{-1}$  (–C–OH); 1,203  $\text{cm}^{-1}$  (–P=O); 1,052, 1,014, and 929  $\text{cm}^{-1}$  (–P–OH). The FTIR spectra of HP-β-CD show absorption bands at: 3,399  $\text{cm}^{-1}$  (O–H stretching vibration); 2,928  $\text{cm}^{-1}$  (C–H stretching); 1,658  $\text{cm}^{-1}$  (–OH bending); 1,331, and 1,373  $\text{cm}^{-1}$  (OH deformation); 1,156 and 1,084  $\text{cm}^{-1}$  (C–O–C stretching and OH banding); 1,035  $\text{cm}^{-1}$  (CH<sub>2</sub>–OH stretching). In the FTIR spectra of inclusion complex, the specific peak of PBTCa portion can not be detected, indicating a strong interaction between the PBTCa and HP-β-CD because of the formation of an inclusion complex. The other peaks of PBTCa are

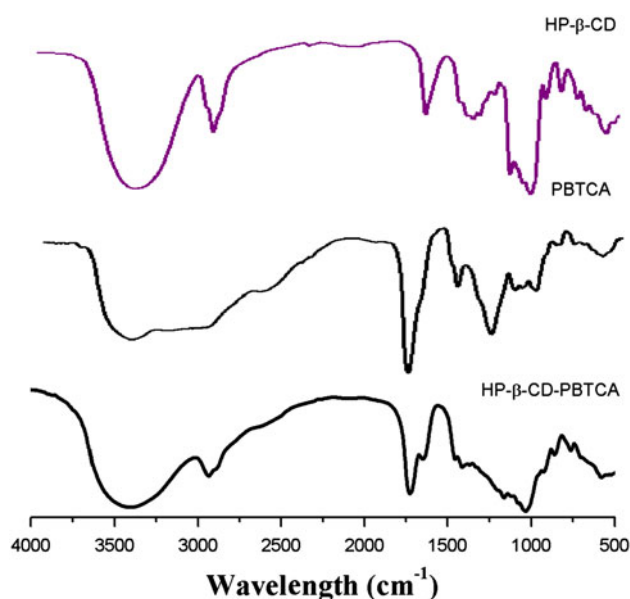


**Fig. 5** FTIR spectra of pure PBTCa, HP-β-CD, and the inclusion complex of PBTCa with HP-β-CD

superposed over HP-β-CDs' peaks. By contrast, however, it can be observed that two moderate intensity spectral absorption peaks at 1,725 and 925  $\text{cm}^{-1}$  close to the specific peak of pure PBTCa at 1,720 and 929  $\text{cm}^{-1}$ , suggesting functional groups portion of PBTCa (–C–O and –P–OH) have likely been penetrated the cavity of HP-β-CD.

Evaluation of inhibition performance of the inclusion complex using EIS

Figures 6 and 7 show the Nyquist diagrams of Q235 carbon steel in 0.1 M H<sub>2</sub>SO<sub>4</sub> at 25 ± 1 °C containing various concentrations of PBTCa and the inclusion complex after 60 min immersion, respectively. All the impedance spectra exhibit one single depressed semicircle, and the diameter of semicircle increases with the increase of PBTCa and the inclusion complex inhibitor concentration, which indicates the corrosion-inhibiting mechanism of the inclusion complex is similar with PBTCa and the impedance of inhibited substrate increases with increase in concentration of the inclusion complex in the corrosive solution. Compared with PBTCa, the greater diameter of semicircle of the inclusion complex at the same concentration shows that the inclusion complex achieves better performance in decreasing corrosive rate.

The EIS parameters, i.e., charge transfer resistance ( $R_t$ ) with inhibitors were calculated by ZView software, as shown in Fig. 8. The values of  $R_t$  calculated from EIS can visually display the inhibition effects of PBTCa and the inclusion complex. The inhibition efficiency ( $\eta_{(EIS)}$ ) was calculated using the charge transfer resistance as Eq. 2 [1].

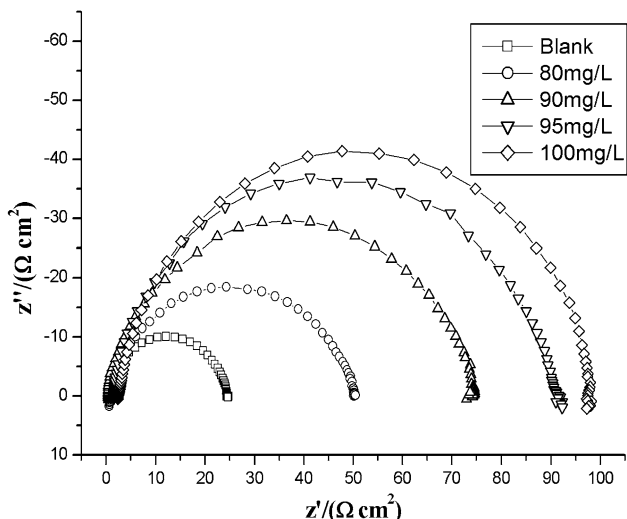


**Fig. 6** Nyquist diagrams of the corrosion of Q235 carbon steel in 0.1 M H<sub>2</sub>SO<sub>4</sub> at 25 ± 1 °C containing various concentrations of PBTCA after 60 min immersion

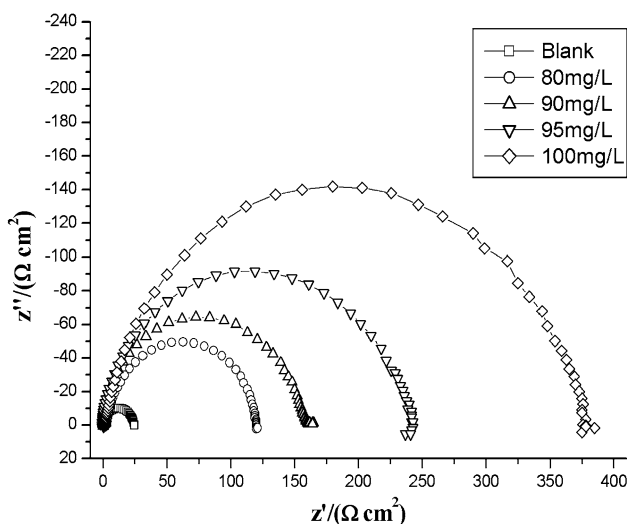


**Fig. 7** Nyquist diagrams of the corrosion of Q235 carbon steel in 0.1 M H<sub>2</sub>SO<sub>4</sub> at 25 ± 1 °C containing various concentrations of the inclusion complex after 60 min immersion

$$\eta_{(EIS)} = \left[ \frac{R_{t(inh)} - R_t}{R_{t(inh)}} \right] \times 100\% \quad (2)$$

where  $R_t$  and  $R_{t(inh)}$  are the charge transfer resistance values without and with an inhibitor, respectively. The inhibition efficiencies calculated from Eq. 2 are presented in Fig. 9. The inclusion complex exhibits the highest inhibition efficiency of 93.49 %. Therefore, the results show the active effect of HP- $\beta$ -CD on enhancing inhibition efficiency of PBTCA, which can be attributed to the formation of the inclusion complex of PBTCA with HP- $\beta$ -CD.

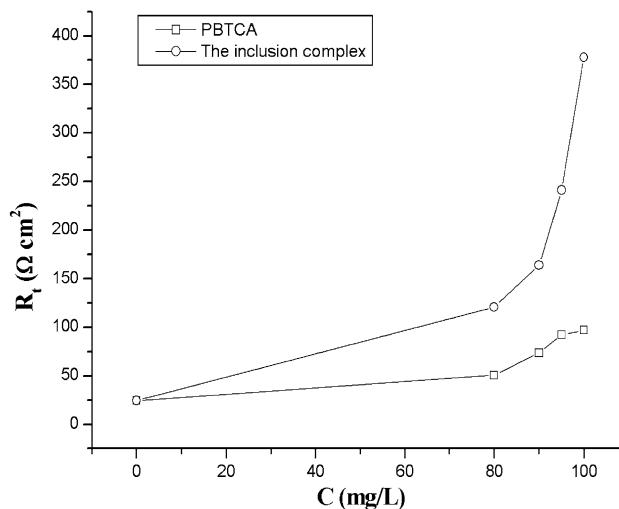


**Fig. 8** Relation between  $R_t$  calculated from Figs. 6 and 7 and concentration

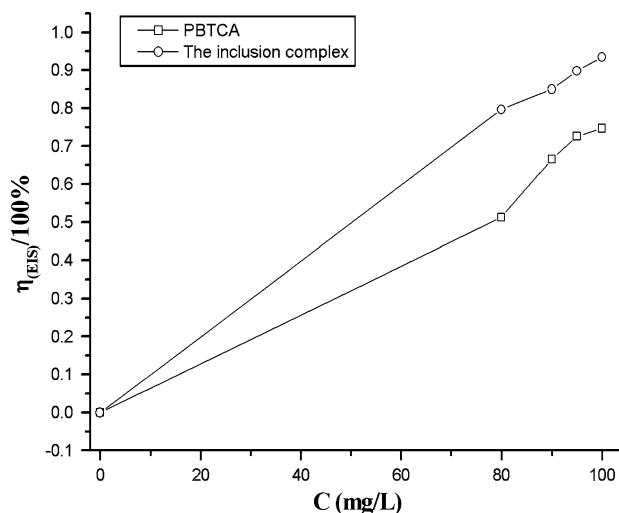


**Fig. 9** Inhibition efficiency calculated from EIS. The maximum inhibition efficiency of PBTCA and the inclusion complex is 74.99 and 93.49 %, respectively

Evaluation of inhibition performance of the inclusion complex using polarization curve

The polarization curve was used to investigate the quality of PBTCA and the inclusion complex on protecting Q235 carbon steel from corrosion in 0.1 M H<sub>2</sub>SO<sub>4</sub> solution at 25 ± 1 °C and the results were shown in Figs. 10, 11, respectively. Electrochemical corrosion parameters, i.e., corrosion current ( $i_{corr}$ ) were obtained by extrapolation of the Tafel lines, as shown in Fig. 12. It could be observed that the corrosion current densities decreased with the addition of PBTCA and the inclusion complex, which may be due to adsorption and complex formation at the metal surface [30–32]. However, corrosion current densities of



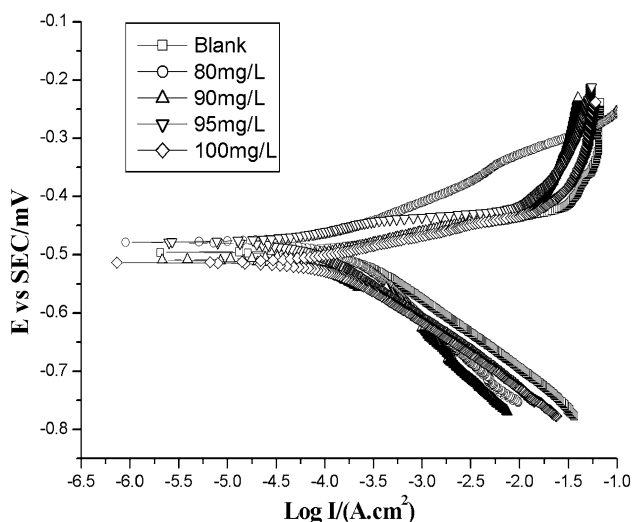


**Fig. 10** Polarization curves of the corrosion of Q235 carbon steel in 0.1 M H<sub>2</sub>SO<sub>4</sub> at 25 ± 1 °C containing various concentrations of PBTCA after 60 min immersion

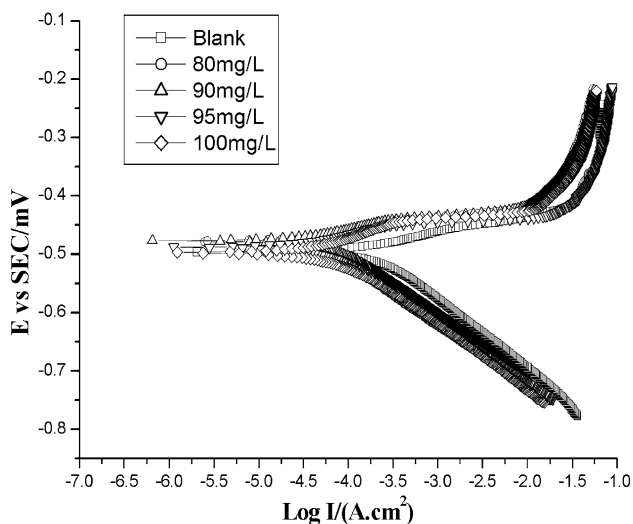


**Fig. 11** Polarization curves of the corrosion of Q235 carbon steel in 0.1 M H<sub>2</sub>SO<sub>4</sub> at 25 ± 1 °C containing various concentrations of the inclusion complex after 60 min immersion

the inclusion complex have the marked tendency to decrease in corrosion media, indicating that formation of the inclusion complex of PBTCA with HP- $\beta$ -CD was favorable to enhancing inhibition efficiency of PBTCA.

The inhibition efficiency calculated from polarization curve ( $\eta_{pc}$ ) could be calculated as following Eq. 3 [1].

$$\eta_{pc} = \left[ \frac{i_{corr(0)} - i_{corr}}{i_{corr(0)}} \right] \times 100\% \quad (3)$$

where  $i_{corr(0)}$  and  $i_{corr}$  are the corrosion current densities without and with an inhibitor, respectively. The values of  $\eta_{pc}$  are shown in Fig. 13 and the inhibition efficiencies calculated from polarization curves show the same trend as those observed from EIS measurements.

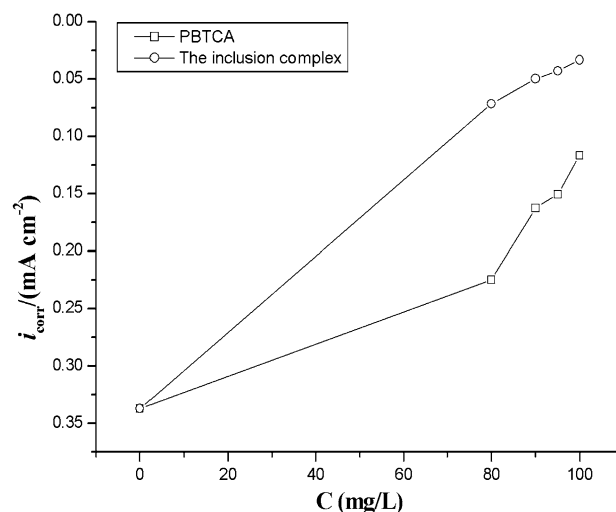


**Fig. 12** Relation between  $i_{corr}$  calculated from Figs. 10 and 11 and concentration

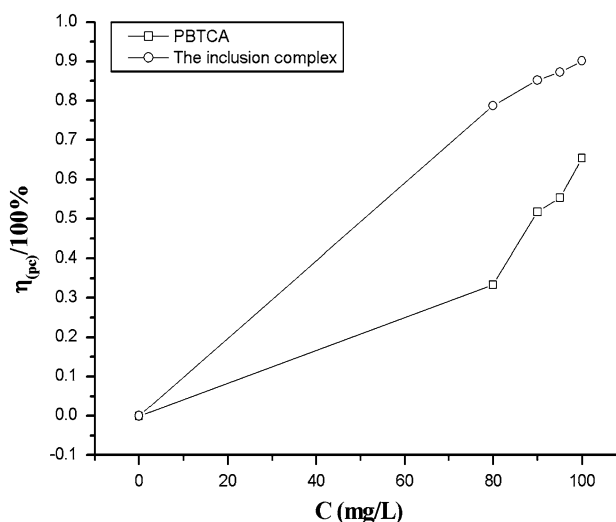


**Fig. 13** Inhibition efficiency calculated from polarization curves. The maximum inhibition efficiency of PBTCA and the inclusion complex is 65.37 and 90.11 %, respectively

Evaluation of inhibition performance of the inclusion complex using SEM

The surface morphological changes on the corroding Q235 carbon steel surface were observed by SEM. Figure 14 shows a SEM photograph recorded for steel samples exposed in 0.1 M H<sub>2</sub>SO<sub>4</sub> solution without and with inhibitors (100 mg/L) at 25 ± 1 °C. In the absence of inhibitors, it can be seen (Fig. 14a) that the steel samples after immersion seem very rough on the surface. However, in the presence of PBTCA (Fig. 14b) and the inclusion complex (Fig. 14c), the rough surface is reduced indicating the inhibition effect of the inclusion complex like PBTCA on the surface of the carbon steel. On the other hand, in the present of the inclusion complex the surface roughness is

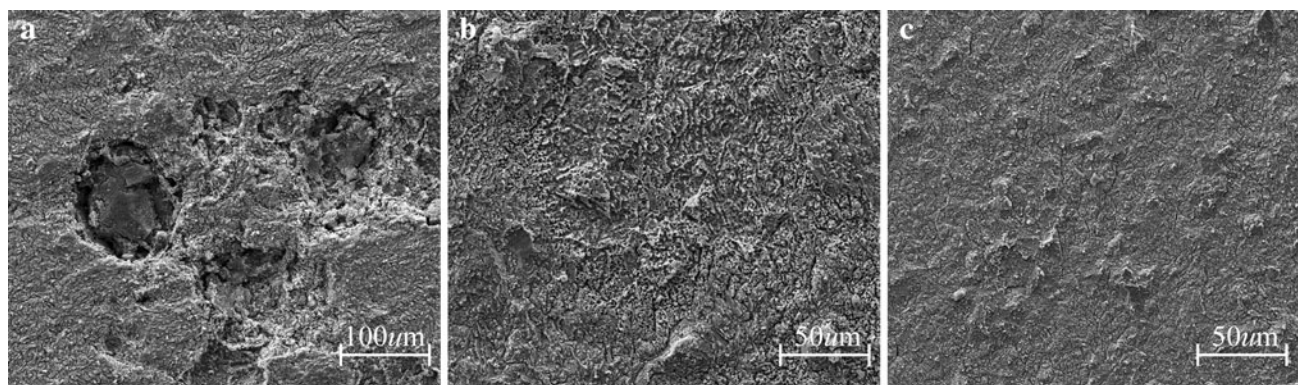


**Fig. 14** SEM photographs of the surface for Q235 carbon steel after 24 h of immersion in 0.1 M H<sub>2</sub>SO<sub>4</sub> at 25 ± 1 °C (a) without, (b) with 100 mg/L of PBTCA, and (c) With 100 mg/L of the inclusion complex

visibly reduced compared to the steel sample in the presence of PBTCA, which shows the formation of stable anti-corrosion films.

## Conclusion

The inclusion complexes of PBTCA with HP- $\beta$ -CD were prepared by freeze drying method. Concerning the formation of the inclusion complex, some important evidences have been obtained from UV-Vis absorption spectrum and FTIR. From UV-Vis spectra, it was observed that the PBTCA characteristic absorption band at 221.5 nm in inclusion complexes was strengthened and the inclusion ratio of HP- $\beta$ -CD with PBTCA is 1:1. FTIR spectra showed that the PBTCA penetrates the HP- $\beta$ -CD cavities and the inclusion complex is stabilized, which may be due to hydrogen bonding between HP- $\beta$ -CD and PBTCA. In addition, the results of EIS and polarization curve studies revealed that the presence of the inclusion complex better achieved the anti-corrosion property in aggressive medium than was the case with alone PBTCA and the highest inhibition efficiency of the inclusion complex over 90 % was obtained. SEM observations of the carbon steel surface confirmed the protective role of the inclusion complex, which may refer to adsorption and complex formation at the metal surface with the inclusion complex.

**Acknowledgments** This work has been supported by the National High Technology Research and Development Program (“863” Program) of China (2007AA11A117) from the Ministry of Science and Technology of China. Financial support of the “863” Program is highly appreciated.

## References

- Zhang, G.C., Ge, J.J., Sun, M.Q., Pan, B.L., Mao, T., Song, Z.Z.: Investigation of scale inhibition mechanisms based on the effect of scale inhibitor on calcium carbonate crystal forms. *Sci. China, Ser. B: Chem.* **55**(1), 114–120 (2007)
- Zhang, W., Lu, X., Liu, Y., Pan, G., Luo, J.: Chemical mechanical polishing of copper in organic phosphonic acid system slurry. Technical Sessions—Proceedings of CIST2008 & ITS-IFTToMM2008 Beijing, China, 906-907 (2008)
- Abulkibash, A., Khaled, M., Elali, B.: Corrosion inhibition of steel in cooling water system by 2-phosphonobutane-1,2,4-tricarboxylic acid and polyvinylpyrrolidone. *Arab. J. Sci. Eng.* **33**(1A), 29–40 (2008)
- Benabdellah, M., Ousslim, A., Hammouti, B., Elidrissi, A., Aouniti, A., Dafali, K., Bekkouch, K., Benkaddour, M.: The effect of poly(vinyl caprolactone-co-vinyl pyridine) and poly(vinyl imidazol-co-vinyl pyridine) on the corrosion of steel in H<sub>3</sub>PO<sub>4</sub> media. *J. Appl. Electrochem.* **37**, 819–826 (2007)
- Al-Sarawy, A.A., Fouda, A.S., Shehab El-Dein, W.A.: Some thiazole derivatives as corrosion inhibitors for carbon steel in acidic medium. *Desalination* **229**, 279–293 (2008)
- Hosseini, M.G., Tavakoli, H., Shahrabi, T.: Synergism in copper corrosion inhibition by sodium dodecylbenzenesulphonate and 2-mercaptobenzimidazole. *J. Appl. Electrochem.* **38**, 1629–1636 (2008)
- Umoren, S.A., Obot, N.I.B., Obi-Egbedi, O.: Raphia hookeri gum as a potential eco-friendly inhibitor for mild steel in sulfuric acid. *J. Mater. Sci.* **44**, 274–279 (2009)
- Hosseini, M.G., Khalilpur, H., Ershad, S., Saghatforoush, L.: Protection of mild steel corrosion with new thia-derivative Salens in 0.5 M H<sub>2</sub>SO<sub>4</sub> solution. *J. Appl. Electrochem.* **40**, 215–223 (2010)
- Fu, J.-J., Li, S.-N., Cao, L.-H., Wang, Y., Yan, L.-H., Lu, L.-D.: L-Tryptophan as green corrosion inhibitor for low carbon steel in hydrochloric acid solution. *J. Mater. Sci.* **45**, 979–986 (2010)
- Gopi, D., Govindaraju, K.M., Kavitha, L.: Investigation of triazole derived Schiff bases as corrosion inhibitors for mild steel in hydrochloric acid medium. *J. Appl. Electrochem.* **40**, 1349–1356 (2010)
- Shah, P.P., Shukla, S.K., Misra, A.N., Patel, D.C.: Scale inhibition in recirculating cooling water system by low concentration of organic inhibitors. *Chem. Eng. World* **28**, 83–86 (1993)
- Rajendran, S., Apparao, B.V., Palaniswamy, N.: Synergistic effect of Zn<sup>2+</sup> and ATMP in corrosion inhibition of mild steel in neutral environment. *Bull. Electrochem.* **12**, 15–19 (1996)
- Rajendran, S., Apparao, B.V., Periasamy, V., Karthikeyan, G., Palaniswamy, N.: Comparison of the corrosion inhibition efficiencies of the ATMP-molybdate system and the ATMP-molybdate-Zn<sup>2+</sup> system. *Anti-Corros. Method. Mater.* **45**, 109–112 (1998)

14. Rajendran, S., Earnest John, P.B.R.E., Peter Pascal, R.A., John, A.A., Sundaravadevelu, A.M.: Influence of chloride ion concentration on the inhibition efficiency of the HEDP-Zn<sup>2+</sup> system. *Trans. SAEST* **38**, 11–15 (2003)
15. Yabuki, A., Kunimoto, H.: Optimum condition of phosphonic acid inhibitor under a flowing solution. *Zairyo to Kankyo/Corrosion Engineering*. **54**, 74–78 (2005)
16. Thi Xuan Hang, T., Truc, T.A., Nam, T.H., Oanh, V.K., Jorcin, J.B., Pèbère, N.: Corrosion protection of carbon steel by an epoxy resin containing organically modified clay. *Surf. Coat. Technol.* **201**, 7408–7415 (2007)
17. Mohanan, S., Maruthamuthu, S., Kalaiselvi, N., Palaniappan, R., Venkatachari, G., Palaniswamy, N., Raghavan, M.: Role of quaternary ammonium compounds and ATMP on biocidal effect and corrosion inhibition of mild steel and copper. *Corros. Rev.* **23**, 425–444 (2005)
18. Thammarat, A., Burkhard, S., Gunter, R.: Crystal structures of  $\beta$ -cyclodextrin complexes with formic acid and acetic acid. *J. Incl. Phenom. Macrocycl. Chem.* **47**, 39–45 (2003)
19. Irina, V.T., Natalya, A.O.: Study on inclusion complex formation of m-aminobenzoic acid with native and substituted  $\beta$ -cyclodextrins. *J. Solution Chem.* **36**, 1167–1176 (2007)
20. Shen, Q., Wu, X.H., Wang, M., Shen, X.Q., Ren, Y., Wu, G.R.: Study on identification and anti-lipid peroxidation effects of  $\beta$ -cyclodextrin inclusion of chlorogenic acid extracted from dandelion. *Food Sci.* **28**, 30–34 (2007)
21. Belyakova, L.A., Varvarin, A.M., Lyashenko, D.Y., Khora, O.V., Oranskaya, E.I.: Complexation in a  $\beta$ -cyclodextrin-salicylic acid system. *J. Colloid.* **69**, 546–551 (2007)
22. Cappello, B., Maio, C., Iervolino, M., Miro, A.: Combined effect of hydroxypropyl methylcellulose and hydroxypropyl- $\beta$ -cyclodextrin on physicochemical and dissolution properties of celecoxib. *J. Incl. Phenom. Macrocycl. Chem.* **57**, 237–244 (2007)
23. Patel, R., Bhimani, D., Patel, J., Patel, D.: Solid-state characterization and dissolution properties of ezetimibe–cyclodextrins inclusion complexes. *J. Incl. Phenom. Macrocycl. Chem.* **60**, 241–251 (2008)
24. Horiuchia, Y., Abea, K., Hirayamaa, F., Uekama, K.: Release control of theophylline by  $\beta$ -cyclodextrin derivatives: hybridizing effect of hydrophilic, hydrophobic and ionizable  $\beta$ -cyclodextrin complexes. *J. Controlled Release* **15**, 177–183 (1991)
25. Hostetlera, J.S., Hansonc, L.H., Stevensa, D.A.: Effect of hydroxypropyl- $\beta$ -cyclodextrin on efficacy of oral itraconazole in disseminated murine cryptococcosis. *J. Antimicrob. Chemother.* **32**, 459–463 (1993)
26. Cserhádi, T., Forgács, E.: Inclusion complex formation of steroidal drugs with hydroxypropyl- $\beta$ -cyclodextrin studied by charge-transfer chromatography. *J. Pharm. Biomed. Anal.* **18**, 179–185 (1998)
27. Zou, C.J., Liao, W.J., Zhang, L., Chen, H.M.: Study on acidizing effect of  $\beta$ -cyclodextrin-PBTCA inclusion compound with sandstone. *J. Petrol. Sci. Eng.* **77**, 219–225 (2011)
28. Ventura, C.A., Giannone, I., Paolino, D., Pistara, V., Corsaro, A., Puglisi, G.: Preparation of celecoxib-dimethyl- $\beta$  cyclodextrin inclusion complex: characterization and in vitro permeation study. *Eur. J. Med. Chem.* **40**, 624–631 (2005)
29. Tong, L.H.: *Cyclodextrin Chemistry-Foundation and Application*. Beijing Science Press, China (2001)
30. Kalman, E.: *Corrosion Inhibitors*. Published for EFC No. 11, Institute of Materials, London. (1999)
31. Gopi, D., Rajeswari, S.: In Proceedings of NACE international conference, corrosion its mitigation and preventive maintenance, Mumbai, India. 435 (2000)
32. Gopi, D., Rajeswari, S.: In Proceedings of tenth national congress on corrosion control conference, Madurai, India. 353 (2000)